Wireless Networks (2022) 28:1923–1934
https://doi.org/10.1007/s11276-022-02922-0

ORIGINAL PAPER

# Generalised asymptotic frame-work for double shadowed $\kappa - \mu$ fading with application to wireless communication and diversity reception

Puspraj Singh Chauhan[1] · Sandeep Kumar[2] · Vipin Kumar Upaddhyay[3] · Sanjay Kumar Soni[3] · Rajan Mishra[3] · Brijesh Kumar[3]

Accepted: 7 February 2022 / Published online: 2 April 2022


## Abstract

In this work, the asymptotic performance analysis over double shadowed $\kappa$-$\mu$ fading channel is presented. More specifically, the unified asymptotic tight performance bounds for maximum ratio combining , selection combining and equal gain combining diversity receptions is presented. The system performance in terms of the outage probability (OP), symbol error probability (SEP) (coherent/non-coherent), the average probability of detection, and the average area under the receiver operating characteristic curve (AUC) is studied. To gain more insights and to validate the asymptotic slope of the results, the coding gain and diversity gain for OP, SEP, probability of missed detection, and complementary AUC for all the diversity techniques are also presented. It is found that the asymptotic slope of all the performance parameters and diversity techniques depend only on the number of multipath clusters and the diversity order of the system. Further, simulation results are presented to demonstrate the effectiveness of the proposed methodology under various channel conditions in diverse field of applications, such as vehicle-to-vehicle communication, wearable communication, and wireless power transfer related technologies .

**Keywords** UAV communication · Bit error rate · Coding gain · Diversity gain

## 1 Introduction

With the diverse nature of applications in 5G and beyond technologies, we are facing the problem of maintaining the required quality of services (QoS) like high data rate and low latency, etc. in various propagation scenarios of unmanned aerial vehicle (UAV) communication, namely ground-to-ground (G2G), air-to-ground (A2G), and air-to-air (A2A) and other wireless applications due to random variation of the received signal strength. This variation in the received signal strength can be characterized in the form of several multipath statistical distributions like Rayleigh, Ricean, Nakagami, Weibull, $\kappa - \mu$, $\eta - \mu$, etc., shadowing distributions like Lognormal, Gamma, and Inverse Gaussian, etc., and more practical fading models which accommodate earlier both phenomena, such as shadowed Weibull, Rician shadowed, etc. [1–10]. The applications of line-of-sight (LOS) and shadowed LOS signal propagation scenarios is found in the UAV assisted communication system both in civil and defence domains [3–6]. In this regard, the performance of UAV aided relay network over $\kappa - \mu$ fading channel has been analyzed in [4]. The secrecy performance of UAV assisted relay cognitive system over Nakagami-m fading channel has been explored in [5]. The performance evaluation of UAV assisted data collection over Ricean/Shadowed fading channel has been studied in [6]. In other works, various composite fading models of LOS and multiplicative shadowing like Hoyt/lognormal [7], Weibull/Lognormal [8], variants of Gamma [9] and Inverse Gaussian [10] with generalized multipath fading models and their special cases.

Recently more generalized double shadowed multipath fading models have been proposed in the literature.

✉ Sanjay Kumar Soni
sanjoo.ksoni@gmail.com; sksoniec@mmmut.ac.in

1 Pranveer Singh Institute of Technology, Kanpur, India

2 Central Research Laboratory Bharat Electronics Limited, Gaziabad, India

3 M. M. M. University of Technology, Gorakhpur, India

Further, it has been shown that these models provide an excellent fit with the field measurement data under various communication scenarios [11]. This model can be characterized when different shadowing levels influence direct propagation of signal, where the received signal is influenced by the second round of shadowing due to moving obstacles in the vicinity of transmitter (Tx) or receiver (Rx). To this extent, double shadowed Ricean (DSR) distribution is reported in [11], where two formats of dual shadowing have been described in details. The novel closed-form mathematical expressions for the probability density function (PDF), cumulative distribution function (CDF), and moment generating function (MGF) have been derived, and the impact of various parameters on the system performance is studied. The work is extended to effective rate analysis in [12], whereas the said channel's physical layer security parameters are examined in [13]. Furthermore, a more generalized double shadowed (DS) multipath fading, namely DS $\kappa - \mu$ fading model, is proposed in [14, 15]. Later, in [16, 17] physical layer statistic in terms of the outage probability (OP) and link layer metric are discussed over the above-stated channel.

Generalized fading models, exhibit difficulty in obtaining the exact analytical expressions of the performance parameters. The analysis over these channels become more complex when the performance improvement techniques like diversity combining are employed [18], as the PDF comprises complex mathematical structures. It has already been stated in [19] that simplicity of the distribution is highly desirable to have neat and clean mathematics. Therefore, asymptotic analysis has received special attention in the recent years. It enables mathematical simplicity, thus providing the valuable insights into the system performance against variation in fading parameters. In this regard, the asymptotic performance evaluation of single and multiple antennas receiver in terms of the outage probability (OP), error rate, the average probability of detection (PD), and the average area under the receiver operating characteristic curve (AUC) over various fading channels has been performed in [18, 20–26]. The high signal-to-noise-ratio (SNR) asymptotic framework for correlated Rayleigh distribution over equal gain combining (EGC) receiver is studied in [20], whereas in [21], the simple closed-form expressions of the performance parameters over Weibull distribution for selection diversity are derived and their significance for practical applications are discussed in details. On a similar line, the simplified mathematical expressions for error rate and OP over correlated Beckmann fading and $\alpha - \mu$ fading for maximum ratio combining (MRC), selection combining (SC), and EGC diversity reception is derived in [22] and [23], respectively. Asymptotic approximation of the OP and bit error rate for different diversity techniques over the Beaulieu-Xie fading channel is provided in [24] and [25]. It has been shown that the closed-form expressions provided in both the works are very tightly bound. The usefulness of the tight bound at high SNR is also demonstrated in the above works. Energy detector performance in terms of average PD, and average AUC at high SNR is studied in [26]. As per the author's comprehension, there is no work related to the asymptotic tight bound analysis of DS $\kappa - \mu$ fading channel with diversity reception in the open literature and yet to be determined.

Motivated by this, we have performed the tight asymptotic performance bound of the digital communication system over the double shadowed fading channel, recently reported in [14]. The results produced here are very simplified and generic. They can also be applied for the direct analysis of various special cases of the DS $\kappa - \mu$ fading channel, as discussed in [14]. The main contributions of this paper are as follows:

- Novel and unified origin PDF is proposed for single-input-single-output (SISO) and single-input-multiple-output (SIMO) DS $\kappa$-$\mu$ propagation channel with MRC, EGC, and SC diversity techniques.
- The performance parameters in terms of OP, symbol error probability (coherent and non-coherent), the average PD, and the average AUC over all the diversity schemes are evaluated. The derived bounds are tight at high SNR.
- To gain more insights and to validate the asymptotic slope of the results, the coding and diversity gains for the above said metrics are also presented.

The residuum of paper is coordinated as follows: In Sect. 2, first different approaches for obtaining asymptotic results are discussed, then following [8] origin PDF for DS $\kappa - \mu$ fading channel is evaluated with employing diversity combining techniques. Performance measures, such as the OP, average SEP, average PD, average AUC, and coding and diversity gains are evaluated in Sect. 3. Comprehensive discussion on the proposed formulations through simulation results are presented in Sect. 4, while essence of the work can be found in Sect. 6.

## 2 Origin PDFs

Traditionally, the evaluation of asymptotic expression for different performance parameters follows multiple approaches:

- Zhang *et al.* [18] have given an approach, where asymptotic results for performance metrics require the density function around origin. This approach is well suited for the PDF structures that has closed-form solutions or simplified functions. But, it becomes tedious in the case of composite PDF that has complex structure when analysis with diversity is employed.

- Another approach given by by Peppas *et al.* [26], first determines the solution for performance metrics, then estimates the functions at high SNR. Sometimes, it does not allow the function estimation due to complex structure of the result and also becomes trivial for diversity analysis if diversity PDF of the distribution is cumbersome to derive. Here, we have presented an alternative approach for composite models that requires the origin PDF (obtained by Taylor series expansion around the origin) of the multipath and then averaging with shadowing using the relation given by $f_Z(z) = \int_0^\infty f_{Z|\zeta}(z;\zeta) f_\zeta(\zeta) d\zeta$ [14, eq. (3)]. And if multiple level of shadowing exist, then apply the above process as many times. It enables clean origin PDF expression which leads to diversity operation quiet smoothly, as stated further in this section. Following the procedure illustrated in [8], the origin PDF for conditioned $\kappa-\mu$ shadowed fading is obtained with the aid of Taylor's series expansion of [14, eq. (4)]

$$f_{Z|\zeta}(z;\zeta) \approx \frac{2\mu^\mu m^m (1+\kappa)^\mu}{\Gamma(\mu)(\mu\kappa+m)^m (\bar{z}\zeta)^{2\mu}} z^{2\mu-1} + O, \tag{1}$$

where $\Gamma(.)$ is the Gamma function, $O$ denotes the higher-order terms, $\mu$ signifies the number for multipath clusters, $\kappa$ denotes the total power ratio of dominant to scattered components, and $m$ is the shape parameter of Nakagami-$m$ distribution. The PDF of Inverse Nakagami-$m$ distribution follows [14, eq. (2)]

$$f_\zeta(\zeta) = \frac{2(m_r-1)^{m_r}}{\Gamma(m_r)\zeta^{2m_r+1}} e^{-\frac{(m_r-1)}{\zeta^2}}, \tag{2}$$

where $m_r$ is the shape parameter, $E[\zeta]=1$, and E[.] is the expectation operator. Averaging (1) with (2) using the relation [14, eq. (3)], will yield an expression for the unconditional density function of DS $\kappa-\mu$ fading

$$f_Z(z)^O \approx \frac{2\mu^\mu m^m (1+\kappa)^\mu}{\Gamma(\mu)(\mu\kappa+m)^m (\bar{z})^{2\mu}} \frac{2(m_r-1)_r^m}{\Gamma(m_r)} z^{2\mu-1} \times \int_0^\infty \zeta^{-2m_r-2\mu-1} e^{-\frac{(m_r-1)}{\zeta^2}} d\zeta. \tag{3}$$

Letting $\zeta^2$=$t$, applying [27, eq. (3.381.4)] allows to obtain the closed-form result for origin DS $\kappa-\mu$ envelop PDF

$$f_Z(z)^O \approx \frac{2\mathcal{A}}{\bar{z}^{2\mu}} z^{2\mu-1}, \tag{4}$$

where $\mathcal{A} = \frac{\mu^\mu (1+\kappa)^\mu m^m}{(\mu\kappa+m)^m B(m_r,\mu)(m_r-1)^\mu}$. By using the variable transformation $z=\sqrt{\frac{\gamma\bar{z}^2}{\bar{\gamma}}}$ in (4), results in the power PDF of DS $\kappa-\mu$ fading channel

$$f_Y(\gamma)^O \approx \frac{\mathcal{A}}{\bar{\gamma}^\mu} \gamma^{\mu-1}. \tag{5}$$

where $\gamma$ denotes the instantaneous SNR and $E[Y]=\bar{\gamma}$. Figure 1, represents multiple shapes of the envelope PDF and its asymptotic behavior for varying $\mu$ and $m_r$. It is noticeable that the slope of asymptotic plots varies only with parameter $\mu$. Keeping $\mu$ constant produces parallel shapes near $z\rightarrow 0$ as depicted in Fig. 1. Multiple antennas are employed in the end-to-end communication network to improve received SNR for maintaining the required QOS. MRC, EGC, and SC are different signal combining techniques usually employed for increasing the system reliability, of which MRC yields maximum gain, followed by EGC and then SC. The derived origin PDFs are independent of summation terms and complex functions; thus diversity PDFs can be evaluated in a convenient manner.

## 2.1 Origin PDF with MRC

The instantaneous output of the MRC combiner having $L$ independent and identically distributed (i.i.d.) branches is given by [8]

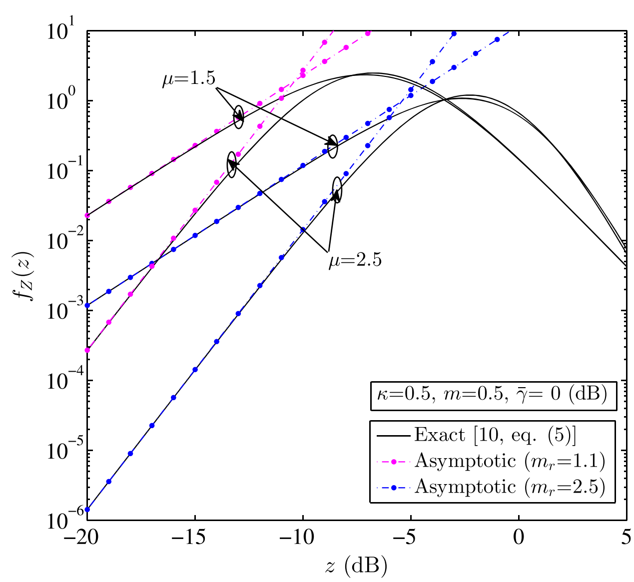


**Fig. 1** PDF plot with exact and asymptotic behaviour for multiple values of $\mu$ and $m$

$$\gamma_{mrc} = \sum_{i=1}^{L} \gamma_i, \tag{6}$$

where $\gamma_i$ signifies the $i^{th}$ branch instantaneous SNR. Assuming average SNR of each branch $\bar{\gamma_1} = \bar{\gamma_2} = \bar{\gamma_3} = \ldots\ldots = \bar{\gamma}$ to be the same, the MGF of $\gamma_{mrc}$ is expressed as [8]

$$M_{\gamma_{mrc}}(s) = (M_\gamma(s))^L, \tag{7}$$

where $M_\gamma(s)$ is the individual branch MGF deduced by taking the Laplace-Transform of (5) with the aid of [27, eq. (3.381.4)], it immediately follows

$$M_\gamma(s) = \frac{\mathcal{A}\Gamma(\mu)}{\bar{\gamma}^\mu s^\mu}. \tag{8}$$

Plugging (8) into (7) and using the relation [27, eq. (3.381.4)], will return the origin PDF with MRC diversity

$$f_Y(\gamma)^O \approx \frac{\mathcal{R}}{\bar{\gamma}^{L\mu}} \gamma^{L\mu-1}, \tag{9}$$

where $\mathcal{R} = \frac{\mathcal{A}^L(\Gamma(\mu))^L}{\Gamma(L\mu)}$.

### 2.2 Origin PDF with EGC

Let $L$ i.i.d. signals are arriving at the receiver equipped with EGC technique, then the output is given as [24]

$$x_{egc} = \sum_{i=1}^{L} \frac{x_i}{\sqrt{L}}, \tag{10}$$

Alike MRC, the MGF for EGC is defined as $M_{x_{egc}} = (M_x(s/\sqrt{L}))^L$. Now, availing the methodology discussed for MRC, the origin PDF will have a similar structure of (9) with $\mathcal{R} = \frac{2^{L-1}\mathcal{A}^L(\Gamma(2\mu))^L(\sqrt{L})^{2L\mu}}{\Gamma(2L\mu)}$.

### 2.3 Origin PDF with SC

Under this scheme, the branch with the highest SNR will be picked, i.e. $\gamma_{sc} = max(\gamma_i)$, $i = 1, 2, \ldots L$. The output instantaneous SNR will have the PDF given by [25]

$$f_{\gamma_{sc}}(\gamma) = L(F_Y(\gamma))^{L-1} f_Y(\gamma), \tag{11}$$

where $F_Y(\gamma) = \frac{\mathcal{A}\gamma^\mu}{\mu\bar{\gamma}^\mu}$ is the CDF of the individual branch and is obtained by putting (5) into the definition $F_Y(\gamma) = \int_0^\gamma f_Y(t)dt$ along with some straight-forward algebraic manipulations. Finally, putting CDF and power PDF expressions into (11), we obtain the origin PDF having a similar structure with parameter $\mathcal{R} = \frac{L\mathcal{A}^L}{\mu^{L-1}}$. Table 1 shows the parameters of diversity PDFs for special cases of DS $\kappa$-$\mu$ fading model.

## 3 Performance measures

Different QoS parameters are used to evaluate the performance of a communication system. The OP, average SEP, average PD, and average AUC are the important performance parameters and are taken in the forefront consideration for designing digital communication systems and cognitive radio networks, respectively. The importance of these performance parameters lies in the fact that the analysis of these performance metrics over different fading channels has been widely studied in the literature.

### 3.1 Outage probability

For wireless communication system with multiple antennas at the receiving section, OP provides the informative response in terms of the probability that the combined received instantaneous SNR is below a specified threshold value $\gamma_{th}$. And if the SNR is above the predefined threshold SNR then transmission quality through channel is better or the impact of channel on the transmission is minimal. Analytically, it is defined as [8]

$$P_{out}(\gamma_{th}) = [Y < \gamma_{th}] = \int_0^{\gamma_{th}} f_Y(\gamma) d\gamma. \tag{12}$$

plugging (9) into (12) and with simple algebraic simplification, we get the simplified expression for the OP given as

$$P_{out}(\gamma_{th}) = \frac{\mathcal{R}\gamma_{th}^{L\mu}}{\bar{\gamma}^{L\mu} L\mu}. \tag{13}$$

Likewise, for other diversity schemes $\mathcal{R}$ can be taken from Sects. 2.2 and 2.3. Similar procedure will acquire for other performance metrics discussed in subsequent subsections.

### 3.2 Average SEP

Average SEP is a measure of the noise performance of the digital communication systems over the fading channels. It depends on the average received SNR and other fading parameters of the channel. The designer's main role is to optimize the system performance while keeping the check on the maximum average SEP that it can afford. In this section, we developed generalized average SEP expressions for coherent as well as non-coherent modulations scheme by assuming DS $\kappa - \mu$ fading channel exposed to Additive White Gaussian Noise (AWGN). In coherent modulation formats, such as quadrature phase shift keying

**Table 1** Parameters for special cases of $\kappa$-$\mu$ double shadowed fading model with diversity reception

| Distribution | $\mathcal{R}_{mrc}$ | $\mathcal{R}_{egc}$ | $\mathcal{R}_{sc}$ | $f_Y(\gamma)$ |
|---|---|---|---|---|
| $\kappa-\mu$/shadowed $m_r \rightarrow \infty$ | $\frac{(\mu^{\mu}m^{m}(1+\kappa)^{\mu})^{L}}{(\mu\kappa+m)^{mL}\Gamma(L\mu)}$ | $\frac{2^{L-1}\mu^{L\mu}m^{Lm}(1+\kappa)^{L\mu}(\Gamma(2\mu))^{L}}{(\Gamma(\mu))^{L}(\mu\kappa+m)^{Lm}\Gamma(2L\mu)}$ | $\frac{L\mu^{L\mu}m^{Lm}(1+\kappa)^{L\mu}}{(\Gamma(\mu))^{L}(\mu\kappa+m)^{Lm}\mu^{L-1}}$ | $\frac{R\gamma^{L\mu-1}}{\bar{\gamma}^{L\mu}}$ |
| $\kappa-\mu$ $m_r \rightarrow \infty, m \rightarrow \infty$ | $\frac{(\mu^{\mu}(1+\kappa)^{L\mu}}{e^{L\mu\kappa}\Gamma(L\mu)}$ | $\frac{2^{L-1}\mu^{L\mu}(1+\kappa)^{L\mu}(\Gamma(2\mu))^{L}}{(\Gamma(\mu))^{L}e^{L\mu\kappa}\Gamma(2L\mu)}$ | $\frac{L\mu^{L\mu}(1+\kappa)^{L\mu}}{\sqrt{\mu}^{L}e^{\kappa\mu L}\mu^{L-1}}$ | |
| DSR $(\mu=1)$ | $\frac{(1+k)^{L}m^{mL}(k+m)^{-mL}}{\Gamma(L)(B(m,m_r))^{L}(m\_r1)^{L}}$ | $\frac{2^{L-1}(1+k)^{L}m^{mL}(k+m)^{-mL}}{\Gamma(2L)(B(m,m_r)(m_r-1))^{L}}$ | $\frac{L(1+k)^{L}m^{mL}(k+m)^{-mL}}{(B(m,m_r)(m_r-1))^{L}}$ | $\frac{R\gamma^{L-1}}{\bar{\gamma}^{L\mu}}$ |
| Rician/shadowed $(\mu=1, m_r \rightarrow \infty)$ | $\frac{(1+k)^{L}m^{mL}}{\Gamma(L)(k+m)^{mL}}$ | $\frac{2^{L-1}(1+k)^{L}m^{mL}}{\Gamma(2L)(k+m)^{mL}}$ | $\frac{L(1+k)^{L}m^{mL}}{\Gamma(L)(k+m)^{mL}}$ | |
| Rician $\mu=1, m_r \rightarrow \infty$ $m \rightarrow \infty$ | $\frac{(1+k)^{L}}{\Gamma(L)e^{Lk}}$ | $\frac{2^{L-1}(1+k)^{L}}{\Gamma(2L)e^{Lk}}$ | $\frac{L(1+k)^{L}}{e^{Lk}}$ | |
| Nakagami- $m$ $m_r \rightarrow \infty, m \rightarrow \infty$ $\kappa \rightarrow 0, m=\mu$ | $\frac{m^{mL}}{\Gamma(L)}$ | $\frac{2^{L-1}m^{mL}(\Gamma(2m))^{L}}{\Gamma(2L)(\Gamma(m))^{L}}$ | $\frac{Lm^{mL}}{(\Gamma(m))^{L}m^{L-1}}$ | $\frac{R\gamma^{Lm-1}}{\bar{\gamma}^{mL}}$ |
| Rayleigh $m_r \rightarrow \infty, m \rightarrow \infty$ $\kappa \rightarrow 0, \mu=1$ | $\frac{1}{\Gamma(L)}$ | $\frac{2^{L-1}}{\Gamma(2L)}$ | L | $\frac{L\gamma^{L-1}}{\bar{\gamma}^{L}}$ |
| One sided Gaussian $m_r \rightarrow \infty, m \rightarrow \infty$ $\kappa \rightarrow 0, \mu=\frac{1}{2}$ | $\frac{\left(\frac{1}{2}\right)^{\frac{L}{2}}}{\Gamma(\frac{L}{2})}$ | $\frac{2^{L-1}}{(2\pi)^{\frac{L}{2}}\Gamma(L)}$ | $\frac{2^{L-1}L}{(2\pi)^{\frac{L}{2}}}$ | $\frac{R\gamma^{\frac{L}{2}-1}}{\bar{\gamma}^{\frac{L}{2}}}$ |

(QPSK), $M$-ary phase shift keying (MPSK), $M$-ary pulse amplitude modulation (MPAM), $M$-ary quadrature amplitude modulation (MQAM), etc. require accurate and continuous tracking of carrier phase at receiver side due to abrupt behavior of the channel. Whereas, non-coherent modulation formats such as differential binary phase shift keying (DBPSK), $M$-ary frequency shift keying (MFSK), etc., does not require such information. Here, generalized average SEP is obtained by considering instantaneous SER $P_e(\gamma)$ subjected to asymptotic $f_Y(\gamma)^O$ PDF, i.e. [8, eq. (12)]

$$\bar{P_e} = \int_0^{\infty} P_e(\gamma) f_Y(\gamma)^O d\gamma. \tag{14}$$

### 3.2.1 Coherent average SEP

There are certain situations where the carrier recovery is possible at the receiver end; in those situations, the coherent modulation techniques are used for the data transmission for better performance gains. For coherent modulation format, general SEP expression can be represented as [28, Eq. (17)]

$$P_e(\gamma) = A_p erfc(\sqrt{(B_p\gamma)}), \tag{15}$$

where constants $A_p$ and $B_p$ are defined in [28, Table I] and erfc(.) is complementary error function. Putting (9) and (15) into (14), setting $\sqrt{B_p\gamma} = t$ and with the aid of [29, Eq. (2.8.2.1)], it insinuates

$$\bar{P_e} \approx \frac{A_P \mathcal{R} \Gamma(L\mu + \frac{1}{2})}{(B_p\bar{\gamma})^{L\mu} L\mu\sqrt{\pi}}. \tag{16}$$

### 3.2.2 Non-coherent average SEP

In most scenarios, the carrier recovery is not possible at the receiver; in that case, the less complex and less performance efficient non-coherent modulation techniques are used for data communication [8, 30, 31]. Non-coherent detection techniques are used in certain applications, such as millimeter wave and land-mobile-communication, etc., in 5G and beyond communications. In this section, we will derive the expressions for non-coherent modulation techniques. The generalized expression for the instantaneous error probability over the non-coherent modulation techniques is given as [8, Eq.(18)]

$$\bar{P_e} = A_n \exp(-B_n\gamma), \tag{17}$$

where the parameters $A_n$ and $B_n$ for different non-coherent modulation schemes are given in [8, Table 2]. Plugging (17) and (9) into (14 ) and using [27, Eq.(3.381.4)], the asymptotic closed-form result for the non-coherent average SEP is deduced as

$$\bar{P_e} \approx \frac{A_n \mathcal{R}\Gamma(L\mu)}{(B_n\bar{\gamma})^{L\mu}}. \quad (18)$$

## 4 Energy detector performance metrics

Limited availability of the spectrum band and requirement of higher data rate in future generation wireless systems adduces a new dimension for the researcher. According to the Federal Communications Commission (FCC) report, bands remain idle most of the time, thus introduce a new path for the efficient utilization of the idle band. Cognitive Radio is the technique that fulfills the job by allocating the unused spectrum of the licensed user, also termed as primary user (PU) to the secondary user (SU) based on the spectrum sensing techniques. In addition, when required, SU has to vacant the spectrum, i.e., not causing any interference to the main user services. Among the available sensing mechanism, energy detection draws much attention due to simplicity and lower implementation cost [9, 10, 32]. The method of cognitive learning and optimization techniques have been applied in many diverse fields like development of an intelligent control system for the wheeled robot [33], development of the inertial navigation control system for the wheeled mobile platform [34] and development of the process for welding fixtures [35] etc.

The parameters used to mechanize the performance of energy detector (ED) are the average PD and the average AUC.

### 4.1 Average PD

The probability of detection ($P_d$) is expressed as a function of average received SNR for a fixed value of the probability of false alarm ($P_f$) or as a function of the probability of false alarm for a fixed value of average received SNR. The $P_d$ and $P_f$ for the additive white Gaussian noise (AWGN) is given by [9, eq. (1)]

$$P_d = (\gamma, \lambda) = P_r[Y > \lambda | H_1] = Q_U(\sqrt{2\gamma}, \sqrt{\lambda}), \quad (19)$$

$$P_f = P_r[Y > \lambda | H_0] = \frac{\Gamma(U, \lambda/2)}{\Gamma(U)}, \quad (20)$$

where $\lambda$ is the predefined system threshold, $U$ is the time bandwidth product, $Q_a()$ is the generalised Marcum-Q function of order $a$, and $\gamma = |h|^2 E_s/N_0$, $h$, $E_s$, and $N_0$ are the instantaneous SNR, channel complex gain, signal energy, one sided noise-power spectral density. The hypothesis $H_0$ and $H_1$ corresponds to the absence and presence of the desired signal, respectively. In the case of practical environments, where fading occurs, the average PD can be evaluated as [32, Eq.(23)]

$$\bar{P_d} = 1 - \int_0^{\lambda} f_Y(y|H_1, \lambda) dy, \quad (21)$$

where

$$f_Y(y|H_1, \lambda) = \frac{1}{2}\int_0^{\infty} \left(\frac{y}{2\gamma}\right)^{\frac{U-1}{2}} \exp\left(-\frac{2\gamma + y}{2}\right) I_{U-1}\sqrt{(2\gamma y)} f_Y(\gamma) d\gamma, \quad (22)$$

where $I_b(.)$ refers the modified Bessel function of order $b$ and kind $1^{st}$. After substituting PDF expression (9) into (22), we obtain

$$f_Y(y|H_1, \lambda) = \frac{1}{2}\left(\frac{y}{2}\right)^{\frac{U-1}{2}} \exp\left(-\frac{y}{2}\right) \frac{\mathcal{R}}{\bar{\gamma}^{L\mu}} \times \int_0^{\infty} \gamma^{L\mu - \frac{U}{2} - \frac{1}{2}} \exp(-\gamma) I_{U-1}\sqrt{(2\gamma y)} dy. \quad (23)$$

Utilizing the identities [27, Eq. (6.643.2)] and [27, Eq.(9.220.2)], it follows

$$f_Y(y|H_1, \lambda) = \frac{\mathcal{R}(\Gamma(L\mu))}{2\Gamma(U)\bar{\gamma}^{L\mu}} \left(\frac{y}{2}\right)^{U-1} {}_1F_1\left(U - L\mu; U; -\frac{y}{2}\right), \quad (24)$$

where ${}_1F_1(.)$ is the confluent hypergeometric function. Further, by substituting (24) into (21) and availing [36, Eq. (1.14.1.7)], yields the final asymptotic expression for average $P_d$

$$\bar{P_d} = 1 - \bar{P_m} \quad (25)$$

where $\bar{P_m}$ is the average probability of missed detection provided as.

$$\bar{P_m} = \frac{\mathcal{R}\Gamma(L\mu)}{U\Gamma(U)\bar{\gamma}^{L\mu}} \left(\frac{\lambda}{2}\right)^U {}_1F_1\left(U - L\mu; U + 1; -\frac{\lambda}{2}\right)$$

.

### 4.2 Average AUC

For applications, that require more than one ED, average $P_d$ is not the optimum metric to analyze the ED performance as the $P_d$ curve may cross each other at specific system parameters. Average AUC is the single figure of merit (SFoM) that serves the purpose and provides fruitful insight, how the performance varies with system parameters. It varies from 0.5 to 1 as threshold changes from 0 to infinity. The expression for average AUC under the considered system is given by [10, eq. (24)]

$$\bar{A} = \frac{1}{2^U\Gamma(U)}\int_0^\infty \lambda^{U-1}\exp\left(-\frac{\lambda}{2}\right)\bar{P_d}d\lambda \tag{26}$$

By substituting (25) in the above expression, it results

$$\bar{A} = \frac{1}{2^U\Gamma(U)}\int_0^\infty \lambda^{U-1}\exp\left(-\frac{\lambda}{2}\right)\left\{1-\frac{\mathcal{R}\Gamma(L\mu)}{\Gamma(U+1)\bar{\gamma}^{L\mu}}\left(\frac{\lambda}{2}\right)^U \times {}_1F_1\left(U-L\mu;U+1;-\frac{\lambda}{2}\right)\right\}d\lambda \tag{27}$$

The following closed-form expression for the average AUC is obtained with the aid of [27, eq. (3.381.4)] and [27, eq.(7.522.9)]

$$\bar{A} = 1-\bar{A}^{comp} \tag{28}$$

where

$$\bar{A}^{comp} = \frac{\mathcal{R}\Gamma(L\mu)\Gamma(2U)}{\Gamma(U)\Gamma(U+1)\bar{\gamma}^{L\mu}}{}_2F_1(U-L\mu,2U;U+1;-1)$$

is the complementary average AUC and ${}_2F_1(.)$ is the gauss hypergeometric function.

## 5 Coding and diversity gain

Coding gain and diversity gain are two key asymptotic parameters that provide meaningful information regarding the system's insights behavior. The diversity gain controls the slope of the asymptotic plots, while the shift of the asymptotic plots is determined by coding gain. The OP, average SEP, the average probability of missed detection, and complementary average AUC at high SNR can be expressed in terms of coding and diversity gains are given as [18]

$$\bar{P_e} \approx \left(G^c_{P_e}\bar{\gamma}\right)^{-G^d_{P_e}};\quad P_{out}(\gamma_{th}) \approx \left(G^c_{OP}\bar{\gamma}\right)^{-G^d_{OP}} \tag{29}$$

where $G^c_{P_e}$, $G^c_{OP}$, $G^d_{P_e}$, and $G^d_{OP}$ are the coding and diversity gains for the probability of error and OP, respectively. Similar to the above, the average probability of missed detection ($\bar{P}_m$) and complementary average AUC ($\hat{A}$) at high SNR is also expressed in terms of coding and diversity gains

$$\bar{P}_m \approx \left(G^c_{Pm}\bar{\gamma}\right)^{-G^d_{Pm}};\quad \hat{A} \approx \left(G^c_{\hat{A}}\bar{\gamma}\right)^{-G^d_{\hat{A}}} \tag{30}$$

where $G^c_{Pm}$, $G^c_{\hat{A}}$, $G^d_{Pm}$, and $G^d_{\hat{A}}$ are the coding and diversity gains for the $\bar{P}_m$ and $\hat{A}$. The expressions for coding and diversity gains for DS $\kappa$-$\mu$ distribution are given by

$$G^c_{Pe^{coh}} = B_p\left(\frac{L\mu\sqrt{\pi}}{A_P\mathcal{R}\Gamma(L\mu+\frac{1}{2})}\right)^{\frac{1}{L\mu}} \tag{31}$$

$$G^c_{Pe^{ncoh}} = \frac{B_n}{(A_n\mathcal{R}\Gamma(L\mu))^{\frac{1}{L\mu}}},\quad G^c_{OP} = \left(\frac{L\mu}{\mathcal{R}\Gamma^{L\mu}_{th}}\right)^{\frac{1}{L\mu}} \tag{32}$$

$$G^c_{Pm} = \left(\frac{\Gamma(U+1)}{\mathcal{R}\Gamma(L\mu)\left(\frac{\lambda}{2}\right)^{\mu}{}_1F_1\left(U-L\mu;U+1;-\frac{\lambda}{2}\right)}\right)^{\frac{1}{L\mu}} \tag{33}$$

$$G^c_{\hat{A}} = \left(\frac{\Gamma(U+1)\Gamma(U)}{\mathcal{R}\Gamma(L\mu)\Gamma(2U){}_2F_1(U-L\mu,2U;U+1;-1)}\right)^{\frac{1}{L\mu}} \tag{34}$$

$$G^d_{P_e} = G^d_{OP} = G^d_{Pm} = G^d_{\hat{A}} = L\mu \tag{35}$$

It is noted that the asymptotic slope of all the performance parameters and diversity techniques are the same and dependent only on the number of multipath clusters and the diversity order of the system. while the shift of the plots are different for different combinations of performance parameters and diversity techniques.

## 6 Results and discussion

The validity of the performance measures derived in the previous sections is justified in this section. Here, we examine the system behavior with respect to fading and system parameters, i.e. $\kappa$, $\mu$, $m$, $m_r$, and multi-branch receiver parameter $L$. More specifically, the impact of different fading and system parameters on a variety of performance metrics, such as the OP, average SEP, average PD, and average AUC is examined. The results are corroborated with their simulations (Monte-Carlo, where $10^6$ samples for DS $\kappa$-$\mu$ random variable are generated) and exact (obtained through numerical integration on the MATLAB platform) counterparts for verifying their accuracy. In order to obtain the expressions for special cases of DS $\kappa$-$\mu$ distribution, acquire $\mathcal{R}$ from Table 1.

OP as a function of average received SNR for different values of the channel parameters is plotted in Fig 2. The accuracy of the asymptotic plots at moderate SNR increases with the increase in $m$ and $m_r$ values and a decrease in the value of the threshold SNR. Further, we observe that for $\mu$ = 2 and $\gamma_{th}$ = 0 (dB) in double shadowed $\kappa-\mu$ case, the OP is $9.0134 \times 10^{-4}$ and $9.0134 \times 10^{-6}$ at 20 (dB) and 30 (dB) SNR, respectively. The slope of the curve is $\log_{10}(9.0134 \times 10^{-4}/9.0134 \times 10^{-6})/\log_{10}(30-20) = \mu L$, which justifies that the theoretical slope is in agreement with the simulation results.

Figure 3 shows the variation of average SEP for various values of diversity order and diversity combining

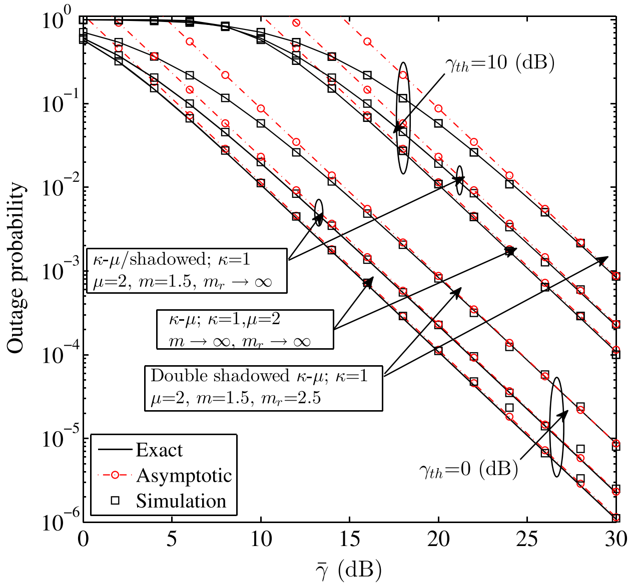


**Fig. 2** Outage probability versus $\bar{\gamma}$ for different special cases of DS $\kappa$-$\mu$ distribution

techniques. The values of the fading parameters considered in the scenario are $\kappa$=2.5, $\mu$=1; $m$=2.5, and $m_r$=2.5. The selected parameters transform DS $\kappa$-$\mu$ fading model to DSR. At $L$=1, the plots of all the combining techniques coincide with each other and at higher values of $L$, MRC gives the best performance, followed by EGC and SC. The slope of the asymptotic plots is verified with the diversity gain, $\mu L$, i.e., for MRC plot at $L$ = 3, the values of SEP are $1.234 \times 10^{-1}$ and $1.234 \times 10^{-5}$ at SNR = 10 (dB) and 20 (dB) respectively, which gives the value of slope as $\log_{10}(1.234 \times 10^{-1}/1.234 \times 10^{-4}))/\log_{10}(20-10)$ = 3.

A comparison of average SEP behaviour of coherent BPSK and non-coherent DBPSK for Nakagami-$m$, as a special case of double shadowed $\kappa$-$\mu$ fading channel is demonstrated in Fig 4. The system performance of BPSK modulation is better than DBPSK modulation as expected and it increases with an increase in the $m$ values. The asymptotic plots show good performance for moderate and high values of average received SNR.

The behavior of missed detection probability as a function of average SNR and for fixed values of false alarm probability for $\kappa$=1, $\mu$=2; $m$=1.5 and $m_r$=2 with SC diversity is plotted in Fig. 5. As can be directly seen from the plots that system performance improves with an increase in $L$ and the probability of false alarm. As observed from the figure, when $\mu$=2 L=2 and $P_f$=$10^{-2}$, the values of missed detection probability at the SNR 20 (dB) and 30 (dB) are $5.672 \times 10^{-2}$ and $5.672 \times 10^{-6}$, respectively. Thus, the asymptotic slope of the plot over 10 (dB) is $\log_{10}(5.672 \times 10^{-2}/5.672 \times 10^{-6})/\log_{10}(30-20)$=4.

Coding gain as a function of the number of multipath cluster at different values of channel parameters is demonstrated in Fig 6 for the OP. It is noted that the coding gain is a decreasing function of $\mu$ and its variation is rapid for initial values of $\mu$ and the variations become marginal for higher values of $\mu$. Moreover, the coding gain increases with the increase in $m$ parameter and a decrease in threshold SNR values .

Since diversity gain is a function of the number of multipath clusters and the diversity order of the system, Fig

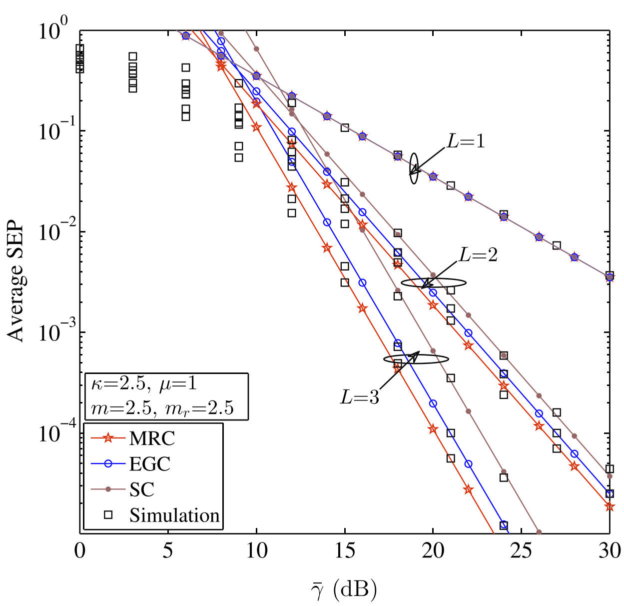


**Fig. 3** Average SEP for coherent $M$-ary PSK versus $\bar{\gamma}$ with constellation size $M$=8

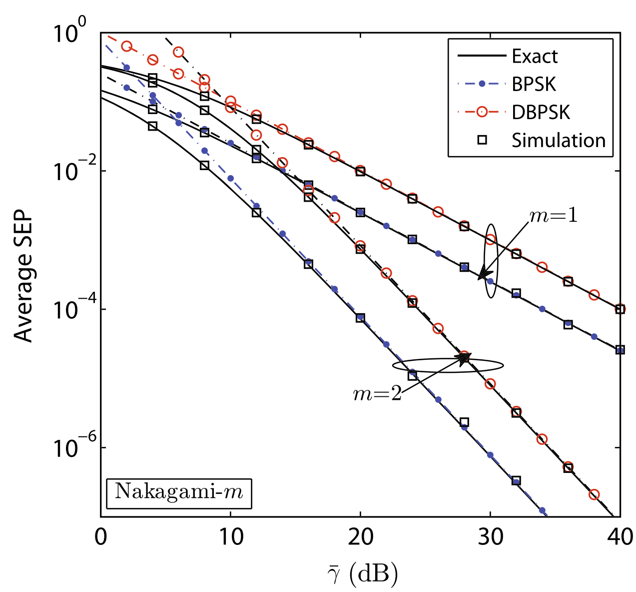


**Fig. 4** Average SEP for coherent and non-coherent binary PSK versus $\bar{\gamma}$ for Nakagami-$m$ distribution

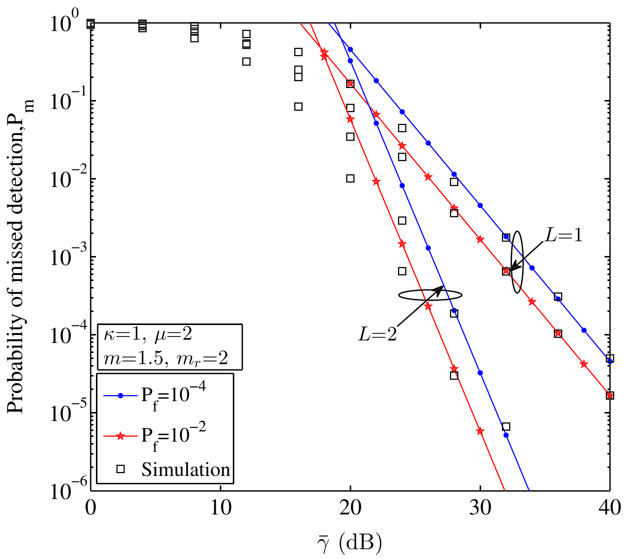


**Fig. 5** Probability of missed detection versus $\bar{\gamma}$ with SC diversity

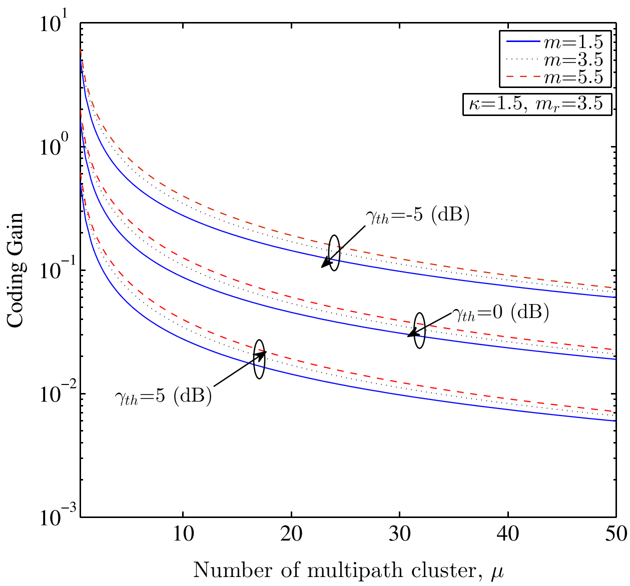


**Fig. 6** Coding gain versus number of multipath cluster $\mu$ for outage probability over double shadowed $\kappa$-$\mu$ fading

7 depicts the behavior of diversity gain for various values of $\mu$ and $L$. Diversity gain increases with the increase in $\mu$ and $L$ values. Interestingly the significant improvement in the system performance is observed for an initial increase in the diversity order and further it becomes marginal. The results produced in this section are very generic and can be directly applied for the design of communication systems where the signal propagation can be modeled in the form of a double shadowed fading channel and its special cases.

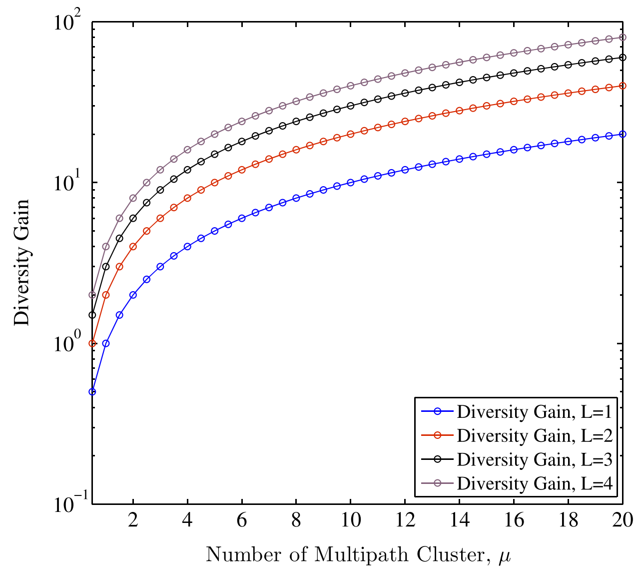


**Fig. 7** Diversity gain versus number of multipath cluster $\mu$ for MRC diversity

## 7 Conclusion

The unified asymptotic analysis over a generalized DS $\kappa - \mu$ composite fading channel is analyzed in this work. The system performance comparison over MRC, SC, and EGC diversity combiner is presented for OP, SEP (coherent/non-coherent). To cater for the spectrum scarcity, the energy detector performance over the said channel is also observed. The derived asymptotic framework is unified and can be used for high SNR applications like Radar and Satellite communications etc. Furthermore, the results produced here are simplified and generic and can also be applied for the direct analysis of various special cases of DS $\kappa - \mu$ composite fading channel. The effect of fading parameters on the system performance is also demonstrated through different plots. To gain more insights and to validate the asymptotic slope of the plots, the coding gain and diversity gain for OP, SEP, and probability of missed detection for all the diversity techniques are presented. It has been found that the asymptotic slope of all the performance parameters and diversity techniques only dependent on the number of multipath clusters and the diversity order of the system. The proposed framework can be suitable for body area network as proposed by Simmons *et al.* [37], where measurement for channel-1 (represent channel between node-1 (Tx at front chest of body-1) and node-3 (Rx at front-centre-waist of body-2) separated by 2 meter) and channel-2 (represent channel between node-3 and node-2 (front-centre-waist of body 1)) is carried at 2.4 GHz in reverberation chamber. At last, we substantiate the accuracy of the proposed framework by comparing them with the Monte-Carlo simulations.

**Acknowledgements** This work is a part of Ministry of Electronics and Information Technology (MeitY), Electronics Systems Development and Application Division, Govt. of India sponsored project entitled "Development of IoT and Drone based Agriculture Monitoring System with Objective of Skill Development of Socially Deprived Community" with Project Ref. No.:26(6)/2019-ESDA .

## References


1. Simon, M. K., & Alouini, M. S. (2004). *Digital communication over fading channels* (2nd ed.). New York: Wiley-IEEE Press.
2. Yacoub, M. (2007). The $\kappa - \mu$ distribution and the $\eta - \mu$ distribution. *IEEE Antennas Propagation Magazine, 49*, 68–81. https://doi.org/10.1109/MAP.2007.370983
3. Khuwaja, A. A., Chen, Y., Zhao, N., Alouini, M., & Dobbins, P. (2018). A Survey of Channel Modeling for UAV Communications. *IEEE Communications Surveys & Tutorials, Fourthquarter, 20*(4), 2804–2821. https://doi.org/10.1109/COMST.2018.2856587
4. Chen, S., Zhang, J., Zeng, W., Peppas, K. P., Ai, B. Performance., & Analysis of Wireless Powered UAV Relaying Systems Over $\kappa - \mu$ Fading Channels. (2018). IEEE Globecom Workshops (GC Wkshps). *Abu Dhabi, United Arab Emirates, 2018*, 1–6. https://doi.org/10.1109/GLOCOMW.2018.8644370
5. Ji, B., Li, Y., Cao, D., Li, C., Mumtaz, S., & Wang, D. (2020). Secrecy performance analysis of uav assisted relay transmission for cognitive network with energy harvesting. *IEEE Transactions on Vehicular Technology, 69*(7), 7404–7415. https://doi.org/10.1109/TVT.2020.2989297
6. Panic, S., Perera, T. D. P., Jayakody, D. N. K., Stefanovic, C., & Prlincevic, B. UAV-assited Wireless Powered Sensor Network over Rician Shadowed Fading Channels 2019. *IEEE International Conference on Microwaves, Antennas, Communications and Electronic Systems (COMCAS), Tel-Aviv, Israel*, 2019: 1-5, https://doi.org/10.1109/COMCAS44984.2019.8958112.
7. Kumar, S., Soni, S., & Jain, P. (2018). Performance of MRC receiver over hoyt-lognormal composite fading channel. *International Journal of Electronics, 105*, 1433–1450. https://doi.org/10.1080/00207217.2018.1460870
8. Chauhan, P. S., Tiwari, D., & Soni, S. K. (2017). New analytical expressions for the performance metrics of wireless communication system over Weibull/Lognormal composite fading. *International Journal of Electronics and Communications, 92*, 397–405. https://doi.org/10.1016/j.aeue.2017.10.013
9. Al-Hmood, H., & Al-Raweshidy, H. S. (2017). Unified modeling of composite $\kappa - \mu$/Gamma, $\eta - \mu$/Gamma and $\alpha - \mu$/Gamma fading channel using a mixture gamma distribution with applications to energy detection. *IEEE Antennas and Wireless Propagation Letters, 16*, 104–108. https://doi.org/10.1109/LAWP.2016.2558455
10. Chauhan, P. S., Negi, P., & Soni, S. K. (2017). A unified approach to modelling of probability of detection over $\alpha - \mu$/IG, $\kappa - \mu$/IG, and $\eta - \mu$/IG composite fading channels with application to cooperative system. *International Journal of Electronics and Communications, 87*, 33–42. https://doi.org/10.1016/j.aeue.2018.01.035
11. Bhargav, N., Silva, C. R. N. D., et al. (2019). Double shadowing the Rician fading model. *IEEE Wireless Communications Letters, 8*, 344–347. https://doi.org/10.1109/LWC.2018.2871677
12. Singh, R., Rawat, M., & Pradhan, P. M. (2020). Effective capacity of wireless networks over double shadowed Rician fading channels. *Wireless Networks, 26*, 1347–1355. https://doi.org/10.1007/s11276-019-02193-2
13. Ai, Y., Kong, L., & Cheffena, M. (2019). Secrecy outage analysis of double shadowed Rician channels. *Electronics Letters, 55*, 765–767. https://doi.org/10.1049/el.2019.0707
14. Bhargav, N., & Silva, C. R. N. D., *et al.* The double shadowed $\kappa - \mu$ fading model.*2019 International Conference on Wireless and Mobile Computing, Networking and Communications (WiMob)*, 2019; Barcelona, Spain: 1-6, https://doi.org/10.1109/WiMOB.2019.8923336
15. Simmons, N., & Silva, C. R. N. D., *et al.* On shadowing the $\kappa - \mu$ fading model.*IEEE Access*, 2020; 8: 120513-120536, https://doi.org/10.1109/ACCESS.2020.3005527.
16. Singh, R., & Rawat, M. Outage analysis of double shadowed $\kappa - \mu$ fading channels.*2019 10th International Conference on Computing, Communication and Networking Technologies (ICCCNT, )*2019, Kanpur, 1-4, https://doi.org/10.1109/ICCCNT45670.2019.8944440.
17. Singh, R., & Rawat, M. On the performance analysis of effective capacity of double shadowed $\kappa - \mu$ fading channels.*IEEE Region 10 Conference (TENCON 2019)*, 2019, 806-810, https://doi.org/10.1109/TENCON.2019.8929632.
18. Wang, Z., & Giannakis, G. B. (2003). A simple and general parameterization quantifying performance in fading channels. *IEEE Transaction on Communications, 51*(8), 1989–1398. https://doi.org/10.1109/TCOMM.2003.815053
19. de Tejerina, G. R., da Silva, C. R. N., & Yacoub, M. D. (2020). Extended $\eta$-$\mu$ fading models. *IEEE Transactions on Wireless Communications, 19*(12), 8153–8164. https://doi.org/10.1109/TWC.2020.3019656
20. Parente, F. R. A., & Santos Filho, J. C. S. (2019). Asymptotically exact framework to approximate sums of positive correlated random variables and application to diversity-combining receivers. *IEEE Wireless Communications Letters, 8*(9), 1012–1015. https://doi.org/10.1109/LWC.2019.2904032
21. Al-Badarneh, Y. H., Georghiades, C. N., & Alouini, M. (2018). Asymptotic performance analysis of the kth best link selection over wireless fading channels: An extreme value theory approach. *IEEE Transaction on Vehicular Technology, 67*(7), 6652–6657. https://doi.org/10.1109/TVT.2018.2798501
22. Zhu, B., Yan, J., Wang, Y., Wu, L., & Cheng, J. (2017). Asymptotically tight performance bounds of diversity receptions over $\alpha - \mu$ fading channels with arbitrary correlation. *IEEE Transaction on Vehicular Technology, 66*(9), 7619–7632. https://doi.org/10.1109/TVT.2017.2686700
23. Zhu, B., Cheng, J., Al-Dhahir, N., & Wu, L. (2016). Asymptotic analysis and tight performance bounds of diversity receptions over beckmann fading channels with arbitrary correlation IEEE transaction on. *Communications, 64*(5), 2220–2234. https://doi.org/10.1109/TCOMM.2016.2543730
24. Olutayo, A., Cheng, J, & Holzman, J. F. Asymptotically tight performance bounds for equal-gain combining over a new correlated fading channel.*15th Canadian Workshop on Inf Theory (CWIT)*, 2017; Quebec City, Canada, 1-5, https://doi.org/10.1109/CWIT.2017.7994814.
25. Olutayo, A., Cheng, J, & Holzman, J. F. Asymptotically tight performance bounds for selection diversity over Beaulieu-Xie fading channels with arbitrary correlation.*IEEE International Conference on Communications (ICC)*, 2017; Paris, France, 1-6, https://doi.org/10.1109/ICC.2017.7997182.
26. Peppas, K. P., Efthymoglou, G., et al. (2015). Energy detection of unknown signals in Gammashadowed Rician fading environments with diversity reception. *IET Communication, 9*(2), 196–210. https://doi.org/10.1049/iet-com.2014.0170
27. Gradshteyn, I. S., & Ryzhik, I. M. (2007). *Table of integrals, series and products* (7th ed.). San Deigo: Academic.
28. Badarneh, O. S., & Aloqlah, M. S. (2016). Performance analysis of digital communication systems over $\alpha - \eta - \mu$ fading

channels. *IEEE Transactions on Vehicular Technology, 65*(10), 7972–81. https://doi.org/10.13140/RG.2.1.4046.7925
29. Prudnikov, A. P., Brychkov, Y., & Marichev, O. I. (1986). *Integrals and series volume 2: special functions* (1st ed.). New York: Gordon and Breach Science Publishers.
30. Chauhan, P. S., & Soni, S. K. (2019). Average SEP and channel capacity analysis over Generic/IG composite fading channels: A unified approach. *Physical Communications, 34*, 9–18. https://doi.org/10.1016/j.phycom.2019.02.003
31. Pant, D., Chauhan, P. S., & Soni, S. K. (2019). Error probability and channel capacity analysis of wireless system over inverse gamma shadowed fading channel with selection diversity. *International Journal of Communication Systems*. https://doi.org/10.1002/dac.4083
32. Chauhan, P. S., Kumar, S., & Soni, S. K. (2019). New approximate expressions of average symbol error probability, probability of detection and AUC with MRC over generic and composite fading channels. *International Journal of Electronics and Communications, 87*, 119–129. https://doi.org/10.1016/j.aeue.2018.11.006
33. Bozek, P., Karavaev, Y. L., Ardentov, A. A., & Yefremov, K. S. (2020). Neural network control of a wheeled mobile robot based on optimal trajectories. *International Journal of Advanced Robotic Systems, 2*, 871.
34. Pirní, R., Hruboš, M., Nemec, D., Mravec, T., & Božek, P. Integration of Inertial Sensor Data into Control of the Mobile Platform. *In Proceedings of the 2015 Federated Conference on Software Development and Object Technologies SDOT 2015. Advances in Intelligent Systems and Computing*, 2017; 511.
35. Semjon, J., Hajduk, M., Jánoš, R., & Vagaš, M. (2013). Modular welding fixtures for robotic cells. *Applied Mechanics and Materials, 309*, 80–87. https://doi.org/10.4028/www.scientific.net/amm.309.80
36. Prudnikov, A. P., Brychkov, Y., & Marichev, O. I. (1986). *Integrals and series volume 3: more special functions* (1st ed.). London: Gordon and Breach Science Publishers.
37. Bhargav, N., Nogueira da Silva, C. R., Cotton S. L., Sofotasios P. C., & Yacoub, M. D. On Shadowing the $\kappa$-$\mu$ Fading Model, http://arxiv.org/abs/Signal Processing, 2018.

**Publisher's Note** Springer Nature remains neutral with regard to jurisdictional claims in published maps and institutional affiliations.

**Puspraj Singh Chauhan** was born in UP, India. He received his Bachelor of Technology in Electronics and Communication Engineering from Uttar Pradesh Technical University, India in 2009, the M Tech degree in Digital Signal Processing from Govind Ballabh Pant Engineering College, Pauri, Uttarakhand, India in 2011. Currently he is working as Assistant Professor at Pranveer Singh Institute Of Technology, Kanpur, U.P., India. He also received best paper award at UPCON 2018, Gorakhpur. His research interests include Wireless Communication and Propagation Channel Modeling

**Sandeep Kumar** received his B. Tech. in electronics and communication from Kurukshetra University, India in 2004 and Master of Engineering in Electronics and Communication from Thapar University, Patiala, India in 2007. He received his Ph.D. from Delhi Technological University, Delhi, India in 2018. He is currently working as Member (Senior Research Staff) at Central Research Laboratory, Bharat Electronics Limited Ghaziabad, India. He has received various awards and certificates of appreciation for his research activities. His research interests include the study of wireless channels, performance modeling of fading channels and cognitive radio networks. He is also serving as a reviewer for IEEE, Elsevier and Springer journals.

**Vipin Kumar Upaddhyay** was born in UP, India. He received his Bachelor of Technology in Electronics and Communication Engineering from Uttar Pradesh Technical University, India in 2012, the M Tech degree in Communication system from Madan Mohan Malaviya University of technology, Gorakhpur, Uttar Pradesh, India. Currently he is working towards the Ph.D. degree in Electronics and Communication Engineering from Madan Mohan Malaviya University of technology, Gorakhpur, Uttar Pradesh, India. His research interests include Wireless Communication and Propagation Channel Modeling, SDR based signal processing.

**Sanjay Kumar Soni** was born in UP, India on March, 1975. He received his Bachelor of Engineering in Electronics Engineering from Madan Mohan Malaviya Engineering College, Gorakhpur, Uttar Pradesh, India in 1997, the M Tech degree in Communication Engineering from IIT Kanpur in 2004, and PhD in wireless Communication Engineering from IIT Kharagpur, India in 2011. Currently he is working as Professor in Electronics and Communication Engineering Department, Madan Mohan Malaviya University of Technology, Gorakhpur, Uttar Pradesh, India. His research interests include Wireless Communication, Propagation Channel Modeling, Cognitive Radio, MIMO-OFDM, UWB Communication, Statistical Characterization of Wireless Channel.

**Rajan Mishra** is Assistant Professor at Department of Electronics and Communication Engineering, Madan Mohan Malaviya University of Technology (Formerly Madan Mohan Malviya Engineering College), Gorakhpur, India since 2009. He received his B.E. degree in Electronics and Communication Engineering from M.J.P. Rohilkhand University, Bareilly, India, M Tech in Digital Systems form Madan Mohan Malaviya Enginneering College, Gorakhpur, India and Ph.D in the field of RF and Microwave from Motilal Nehru National Institute of Technology, Allahabad (Prayagraj) in years 2001, 2007 and 2018 respectively. He has organized several workshops, short term courses and conferences. He is currently working as a Principal Investigator and Co-Chief Investigator in various funded projects. His research interest includes antenna and antenna arrays for medical applications, IOT for agriculture and healthcare sectors.

**Brijesh Kumar** earned a B.Tech. in Electronics Engineering in 1999 at Bundelkhand Institute Engineering and Technology, Jhansi (UP) India; and M.Tech. in VLSI Design in 2009 at UP Technical University, Lucknow, India; and a Ph.D. at Indian Institute of Technology (IIT) Roorkee, India in 2014. He has more than hundred and forty (140) international, national and conference publications in reputed journals and conferences. Currently is working as Professor at Madan Mohan Malaviya University of Technology, Gorakhpur. He has more than 20 years of experience in the field of research and academic. He has received various awards and certificates of appreciation for his academic and research activities. He is a reviewer of many international journals belonging to various organizations and publishers, including IET, IEEE, Taylor & Francis Elsevier, and Springer. He has also served as organizing chair, co-chair, technical chair, and invited speaker at many reputed international and national conferences. He is a member of many expert committees constituted by government and non-government organizations. His research interest includes microelectronics, organic electronics, organic devices, and circuits, VLSI design and technology, novel device structures.